

An Electromyography-driven Central Pattern Generator Model for Robotic Control Application

Kui Xiang, Shuxiang Guo, Zhibin Song

Abstract—Central pattern generator (CPG) models have been designed at abstract levels of the rhythm phenomena and widely applied in robot control. The robot controlled with a CPG model is hard to perceive and respond to the motion intention coming from human beings. A new CPG model driven by surface electromyography (sEMG) was presented in this paper to manipulate robots more favorably without loss of their autonomous capability. The CPG model was designed based on an echo state network (ESN) which was a large, random, recurrent neural network. The frequency modulating from inputs to outputs was researched in this study. It was illustrated that ESNs could learn and generalize the frequency transition pattern. The flexion and extension motion of forearms and the sEMG at biceps and triceps muscles were sampled as the teacher signals to train the CPG model. The prediction error of the trained model was analyzed carefully and the model output was applied to control a rehabilitation exoskeleton. Finally, the future work was discussed on the model structure optimizing.

I. INTRODUCTION

CENTRAL pattern generators (CPGs) [1] are neuronal circuits in peripheral nervous systems that can be activated to produce rhythmic motor patterns such as walking, breathing, chewing, digesting, even speaking and writing. CPGs are able to automatically operate without any sensory inputs and persistently output motor commands. CPGs under the control of higher brain centers are adaptive to environment perturbations. These general principals on CPGs have already been testified in the study of invertebrates and vertebrates.

CPGs bring many inspirations for robot research and lead to many interesting interactions between two fields [2]. CPG models are increasingly used in robotic communities to control different types of robots and different modes of locomotion. For instances: hexapod and octopod robots, swimming robots, quadruped walking control, humanoid robots and etc. CPG models exhibit limit cycle behavior with a few control parameters, so they are suited for distributed implementation and can be entrained with sensory feedback

signals.

CPG models have been designed at several abstract levels of the rhythmic phenomena under study. The neuron models [3] and connectionist models [4] root in micro biology phenomena and try to provide simple and reasonable explanations. Oscillator models [5] focus on population dynamics based on mathematical models of coupled nonlinear oscillators. Phase-locking between those oscillators generates complex motion patterns being able to apply in robot control. Such motion controls are often restricted to low dimensional motions because of the complexity limitation of the models. A new CPG implementation based on deep belief nets was presented to generate high dimensional human motions with unsupervised learning [6].

Recently, an echo state network (ESN) pattern generator was developed to capture the high dimensional nature of CPGs. Moreover, it could be modulated along control dimensions [7]. ESN, liquid state machines and back-propagation decorrelation were unified as reservoir computing, which was widely applied in autonomous robot localization, map, path plan and navigation [8, 9]. Wyffels and et al [10] designed a CPG model based on ESNs to learn the human motion data from CMU Graphics Lab Motion Capture Database [11]. The resulting system was able to generate human motions with multi-DOF and robust against perturbations. Waegeman and et al [12] improved the CPG model in reference [10] to generate both rhythmic and discrete patterns. A limit cycle attractor and a fixed point attractor were embedded in one ESN as the projection of rhythmic motions and discrete motions, respectively.

A robot controlled by CPG models has autonomous behavior modes, but it can not perceive the intentions coming from human beings. If human motion intentions are exacted as the driving signal of CPG models, the robot can actively response to human actions, or be commanded and manipulated by human beings. In fact, the chemical downward neuronmodulators supervise the CPG in spinal cords to match the phase of neural controllers with the body dynamics. Pitti and et al [13] replicated this control strategy based on phase synchronization as an implement of neuromodulators to employ in robot control. Ronsse and et al [14] designed an adaptive oscillator able to observe and track the frequency and phase of input signals synchronously. The elbow position was acquired as input signal to drive the adaptive oscillator and control an assistive exoskeleton.

Based on the above discussion, a conclusion can be drawn that a data-driven CPG model is accord with the

This work was supported by National Natural Science Foundation of China (Grant No. 61101022) and self-determined and innovative research funds of WUT.

K. Xiang is with School of Automation, Wuhan University of Technology, Wuhan 430070, China (e-mail: xkarcher@126.com).

S. Guo is with Dept. of Intelligent Mechanical Systems Eng'g, Kagawa University, Hayashi-cho, Takamatsu 761-0396, Japan (e-mail: guo@eng.kagawa-u.ac.jp).

Z. Song is with Dept. of Intelligent Mechanical Systems Eng'g, Kagawa University, Hayashi-cho, Takamatsu 761-0396, Japan (e-mail: song@eng.kagawa-u.ac.jp).

neurophysiology principle and can lead to better control of robots especially in human-robot interaction. In this study, surface electromyography (sEMG) signals are considered as the driving input of CPG models. SEMG is the common candidate for motion intention recognition and often applied in all kinds of human-robot interfaces. Cavallaro and et al [15] mapped sEMG signals with a neuron-musculo-skeletal model as joint torques to directly control exoskeletons. Fukuda and et al [16] acquired the sEMG signal from a group of muscles to identify the joint positions for prosthesis control. Artemiadis and et al [17] extracted the time varying features of sEMG signals as muscle activations to identify a state space model for robot control. Zhang and et al [18] entrained the neural oscillator reciprocally with sEMG signals to adaptively shape the functional electrical stimulation pattern and suppress the joint tremor. The model in reference [18] is in fact a type of CPG driven by EMG.

Oriented to the control issue of robots especially exoskeletons, a new CPG model driven by EMG is presented in this study based on an ESN. While a robot is endowed with autonomous capability by our CPG model, it is also under the control of human motor commands because the embedded CPG is driven by sEMG signals. In section II, the modeling method will be described in detail, and two typical examples are analyzed in section III. Final is the conclusion.

II. METHODS

A. Basic structure of ESN

The core of ESNs is a large, random, recurrent neural network as an excitable medium which is like a reservoir as shown in Fig.1. The reservoir is able to reserve a high-dimensional collection of nonlinear states $x_i(t)$ influenced by input signals $u(t)$, and any desired output $y(t)$ can be combined by training output function with a simple learning algorithm. ESNs were firstly presented by Jaeger and et al [19] in 2004, and a leaky-integrator version was built in 2007 to learn slow features [20]. ESNs have the ability to process temporal patterns in a fashion similar to the real biology network, so they are pursued by robot communities to imitate human behavior.

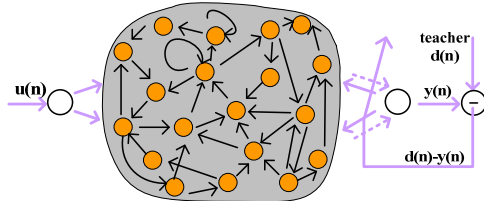


Fig. 1 ESN schema (from reference [19])

A typical ESN has a K -dimensional external input $\mathbf{u}(t)$, N -dimensional reservoir activation state $\mathbf{x}(t)$ and L -dimensional output vector $\mathbf{y}(t)$. At least three connection weight matrices are necessary: input matrix \mathbf{W}^{in} , internal matrix \mathbf{W} and output matrix \mathbf{W}^{out} . The output feedback matrix \mathbf{W}^{fb} is optional. The continuous-time version of an ESN is defined by

$$\dot{\mathbf{x}} = \frac{1}{c} (-a\mathbf{x} + f(\mathbf{W}^{\text{in}}\mathbf{u} + \mathbf{W}\mathbf{x} + \mathbf{W}^{\text{fb}}\mathbf{y})), \quad (1)$$

$$\mathbf{y} = g(\mathbf{W}^{\text{out}}[\mathbf{x}; \mathbf{u}]), \quad (2)$$

where $c > 0$ is a time constant, $a > 0$ is leaking rate, f is a sigmoid function and g is the output activation function. The input \mathbf{u} includes both the sequence from users and a constant bias. When the modeling target is time series, only the bias is preserved. All the weights in matrices \mathbf{W}^* are randomly created in $[0, 1]$. The internal matrix \mathbf{W} needs to be rescaled such that its largest eigenvalue is smaller than 1. During training process, only output matrix \mathbf{W}^{out} is reset using standard linear regression algorithms.

The equation (1) and (2) have discrete versions:

$$\mathbf{x}(n+1) = (1-a)\mathbf{x}(n) + f(s^{\text{in}}\mathbf{W}^{\text{in}}\mathbf{u}(n+1) + \rho\mathbf{W}\mathbf{x}(n) + s^{\text{fb}}\mathbf{W}^{\text{fb}}\mathbf{y}(n) + s^v\mathbf{v}(n+1)), \quad (3)$$

$$\mathbf{y}(n) = g(\mathbf{W}^{\text{out}}[\mathbf{x}(n); \mathbf{u}(n)]), \quad (4)$$

where s^{in} , s^{fb} are the scalings of the input and output feedback, v is normalized noise vector with scaling s^v playing an important role in stabilizing gradient descent optimization. ρ is a compound gain condensed by the time constant c and the stepsize δ in Euler method. ρ and a together determine the effective spectral radius $|\lambda_{\text{max}}|$ of the reservoir weight matrix. When $\rho \leq a$, $|\lambda_{\text{max}}| < 1$ is guaranteed, and the ESN is stable. The typical spectral radius is tuned very close to 1, such that the ESN operates at the edge of chaos where it has greatest predictive power. s^{fb} is set as 0 because nonzero out feedback may result in instability of ESNs. The dimension N of internal matrix determines the modeling capacity, and from the rule of thumb N should be about one tenth of the length of the training sequence.

B. CPG model designing and training

EMG is a zero-mean random stochastic process whose standard deviation is proportional to the active strength of motor units. The sEMG signals measured on the muscle surface provide insight into musculoskeletal systems such as joint angles and torque estimation, muscle fatigue evaluation. The processing methods of sEMG signals have been researched in time [21] and frequency [22] domains for a long time. In this study, only amplitude estimation was considered to acquire a smooth input for CPG models.

A data processing approach with six sequential stages was used to estimate sEMG amplitude in terms of the reference [21]. The six stages are: (1) noise rejection/filtering; (2) whitening; (3) multiple-channel combination; (4) demodulation; (5) smoothing; and (6) relinearization. The estimating process was discussed in the next section. The shape of the sEMG amplitude recorded during an entire action of limbs looks like a bell. The peak of the bell shape is corresponding to the largest torque point. Taking the flexion and extension of forearms as examples, the largest amplitude of biceps muscles appears at about 90 degree of elbow flexion which is also the largest torque point. In words, the sEMG amplitude shape contains enough force information for

driving CPG models.

While sampling sEMG signals, the position, velocity or acceleration signals of joints were synchronously recorded as the observation of human motions. These signals would be used as the input and output of CPG model training. An intuitive structure for CPG models was design as Fig. 2. The sEMG amplitude estimation was inputted into the reservoir of an ESN, and the motions as teacher signals were imposed on the output of the reservoir. According to statistical leaning theory, the dimension of inputs should be not smaller than that of outputs. The human motion works in redundant pattern, and the number of muscles concerned with one specified action is often more than the DOFs of the action itself. The muscles must be selected beforehand to record sEMG signals in terms of the actions that need to be learned. For example, the flexion and extension of forearms depend on biceps and triceps muscles, so at least two channels of sEMG signals should be recorded to learn the flexion and extension motions.

The training method of a CPG model follows the standard of ESNs. Both the input and the output need to be normalized to $[0, 1]$ at first. The matrix \mathbf{W}^{in} and \mathbf{W}^{out} are initialized and their dimension should be in accord with the dimension of inputs and outputs. The dimension of the matrix \mathbf{W} lies on our expectation to the prediction capability of CPG model. Tens of dimensions of internal matrix \mathbf{W} can satisfy the usual demand and an over bulky \mathbf{W} increases computation burden more than prediction effect.

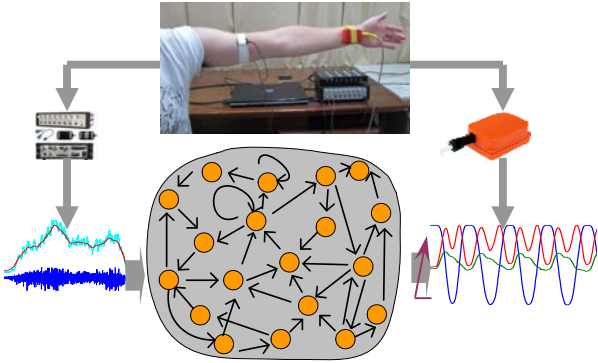


Fig. 2 A CPG model driven by sEMG signals

The input and output signals are introduced into equation (3) point by point, and the echo state $\mathbf{x}(n)$ is updated step by step along with the iterative computation of equation (3). When the training process is over, the complex dynamics between the input and the output is captured as $\mathbf{x}(n)$. The deviation between the output in equation (4) and the real output signals is computed to estimate the weights of the matrix \mathbf{W}^{out} . The weight estimation is very easy with wiener-hopf, recursive least square, ridge regression or sparse regression.

Except the parameter choices, the ESN predictive effect also depends on the cycles contained in the training data. A cycle means an entire action, and the number of the cycles is the effective training length. When the cycles are given, more

intensive samples have little meaning for training effect. In fact, the high sampling rate may import high-frequency noise being harmful to ESNs. ESNs prefer to low sampling rate as far as not too much loss of necessary information. In this study, the sampling frequency of sEMG signals is about 1000Hz, but the amplitude estimation is down resampled to 10Hz as the ESN input.

The prototype in Fig. 2 can be considered as one implementation of CPGs, because ESNs have several properties similar to CPGs. ESNs can work like oscillators only with a constant bias input, and they operate at the edge of chaos, a border between the stable and unstable dynamic regime. The dynamic behavior of ESNs is far more complex than the traditional limit cycle model and its complexity is easily adjusted with a simple parameter, spectral radius $|\lambda_{\text{max}}|$. ESNs can output any high dimensional motion signals for different limbs as long as these limbs' motions are learned beforehand. The behaviors of CPGs can be controlled by simple top-down signals from central nervous system, and the CPG model in Fig. 2 is also driven by sEMG signals.

In order to become a model perfectly identical with CPGs, The training data for ESNs need to be carefully designed and prepared. Only by learning and capturing the dynamics contained in the training data, ESNs can imitate the behaviors similar to CPGs. Waegeman and et al [12] added a random sized padding of the last example value to train a discrete motion, and the output of the ESN learned the transients of the writing motions. Li and et al [11] introduced error feedbacks, such as shift, amplitude and frequency, to modify the states of neurons in the reservoir.

In this study, the variable frequency was specially designed and introduced in training data to improve the adaptive ability of ESNs. As we know, CPGs can output motion pattern with different frequencies wanted by the human himself, and the frequency adaptation similar to CPGs is also expected in ESNs. The smooth frequency transient involved in inputs could help ESNs to obtain the frequency adaptation, but the input with a single frequency could not. An example will be shown in the next section to illustrate such adaptation. The dynamics hidden in the frequency transient is captured by ESNs, and the transient not experienced before is also understood and responded nicely. In this study ESNs were proved to have good generalization in frequency transient, which was very important to CPG models.

III. EXPERIMENTS

A. Walking pattern training driven by sine signals

A group of motion capture data No. 132 was downloaded from the database built by Carnegie Mellon University [11]. The videos were already transformed to bvh file, a type of open text format. The hierarchy skeletons and the motion data were loaded and parsed with our own C++ program. The data No. 132 includes 56 times of independent motion captures. One section of data No. 132-43, which was the walking with

swing shoulders, was selected for our CPG model training. The data No. 132-43 includes about 3 entire gait cycles but it is far away from the training length needs for ESNs. One gait cycle was intercepted and artificially repeated for about 500 times. The cycle selected includes 178 frames of samples, so a sine waveform $u=\sin(2\pi t/178)$ ($t=1, 2, \dots$) was designed as the input for CPG model. There are 31 joints in the data No. 132-43 and each joint has x, y and z position coordinates. So the output data used for training are 93 dimensions and the inputs are 2 dimensions, a sine waveform and a constant bias.

In order to study the frequency transient problem mentioned in section II, a slower-driving signal $u^{\text{slow}}=\sin(2\pi t/(178\times 2))$ was specially designed and alternately aligned with the standard input signal $\sin(2\pi t/178)$ together. Correspondingly, the output signals were resampled and aligned in terms of the same assignment. A 30-dimension internal matrix was assigned for the ESN and the spectrum radius was 0.98. The regular training process of ESNs was carried out and a trained CPG model was obtained waiting for test. A new signal $u^{\text{test}}=\sin(2\pi t/(178\times 1.5))$ was designed to test our CPG model. An input sequence was arranged as $(u, u, u^{\text{test}}, u^{\text{test}}, u, u)$ to test the frequency adaptation. The output of the CPG model was shown in Fig. 3. Only the 1st and 16th dimension of the output were shown for simplicity's sake, and they were the x coordinate of the joints named "Hips" and "LeftFoot", respectively.

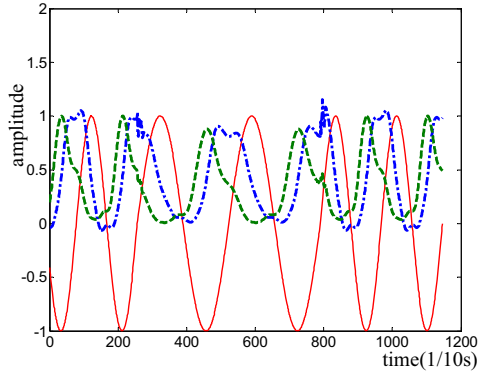


Fig. 3 The frequency transition being trained
(The red solid line: input; the blue dash-dot line: the 1st dimensional output; the green dot line: the 16th dimensional output)

From Fig. 3, a direct conclusion was drawn: the CPG model can realize the frequency transition and re-lock the phase when the frequency of input signals changed. This experiment illustrated that CPG models can learn and adapt the frequency transition by training. The transition between u and u^{test} was not same as that of u and u^{slow} , which proved the generalization ability of ESNs again. When an ESN learns a standard pattern and a slow pattern, any other pattern between them can be realized automatically.

A faster signal $u^{\text{fast}}=\sin(2\pi t/(178\times 0.5))$ was designed and the new input sequence $(u^{\text{slow}}, u^{\text{slow}}, u, u, u^{\text{fast}}, u^{\text{fast}})$ were arranged to test the CPG model further more. The output was shown in Fig. 4. In Fig. 4, a little amplitude oscillation occurred at the transition point from u^{slow} to u , and the similar

phenomenon was in Fig. 3. Considering that the transition from u^{slow} to u was already learned in training, it can be concluded that such amplitude oscillation rooted in the poor smoothness during transition. The signal u^{slow} and u were connected rigidly without any smoothing, and a gradual and smooth transition may avoid the oscillation. The large amplitude oscillation at the transition from u to u^{fast} can not be fully ascribed to the lack of smoothness. In our opinion, the main reason was the absence of the faster pattern from the training.

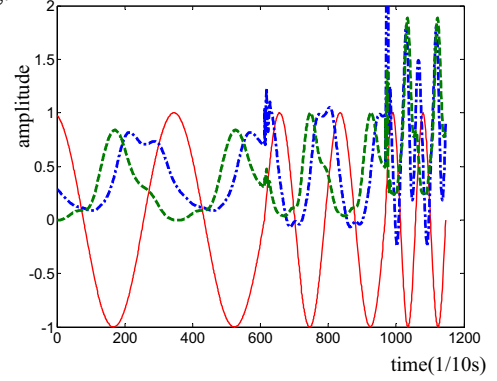


Fig. 4 The frequency transition not being trained
(The red solid line: input; the blue dash-dot line: the 1st dimensional output; the green dot line: the 16th dimensional output)

B. Flexion and extension pattern training driven by sEMG signals

The flexion and extension of forearms were used to training our CPG model. A motion sensor MTx of MTS Systems Co. was laid on the wrist to record the position information. The acceleration and position were read out through a serial communication port. Only the position information was used in this study. The sampling rate predefined in the MTx was 100Hz. There were three types of position expression provided in MTx: Euler angle, rotation matrix and quaternion. The quaternion expression was selected because it could be averaged or interpolated. The first 100 samples were averaged as the initial position. Supposing the offset from the sensor MTx to the rotating center at the elbow was about 300mm, the x, y and z coordinates could be computed of any positions based the quaternion recorded.

Two electrodes were pasted on the biceps and triceps muscles to acquire sEMG signals, respectively. The special instruments from Oisaka Electronic Equipment Ltd were linked with the electrodes to amplify the sEMG signal and remove the noise. An AD sampling board of Advantech Co. Ltd was used to sample the sEMG signals with 1000Hz. A notch filter was applied to remove the power line interference and a band pass filter with frequency 40~150Hz for removing the high and low frequency noise. The amplitude estimation was finished with the six stages mentioned in section II and the related computation items were described in the reference [21]. The amplitude estimation was smoothed with a Kalman filter to omit some unimportant details.

The position and sEMG data were synchronously sampled for about 150s, and 29 entire cycles were intercepted as teacher signals. These signals were repeated to obtain about 1000 cycles. The teacher signals were resampled to 10Hz and then smoothed with a Kalman filter again. The sEMG amplitude estimation and a constant bias were combined as the input for the CPG model and the position coordinates as the output. The 95% data at the front was used for training and the remain for testing. The internal matrix of the ESN was set to be 30 dimensions and the spectrum radius was 0.98. A regular training was finished and the training errors were 0.239, 0.496 and 0.391 on x, y and z coordinate. The test results were shown in Fig. 5 and the test errors were 0.235, 0.494 and 0.385.

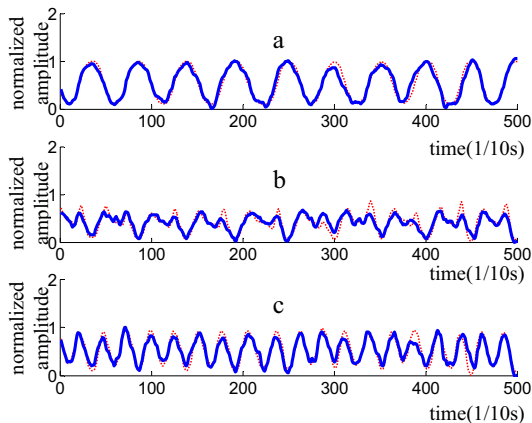


Fig. 5 The output of our CPG model driven by sEMG signals (The curve a, b and c are x, y and z coordinate, respectively. The red dot line: the output expected; the blue solid line: the output predicted)

The coordinates were transformed to the angles at sagittal plane and shown in Fig. 6, and the prediction error was 0.888. Comparing the joint angles expected, the output angles predicted had little different in the amplitude. It was troublesome that there were some phase differences which were hard to be detected in Fig. 5. In terms of synchronization between human and robots, the phase difference was crucial and should be decreased as much as we can.

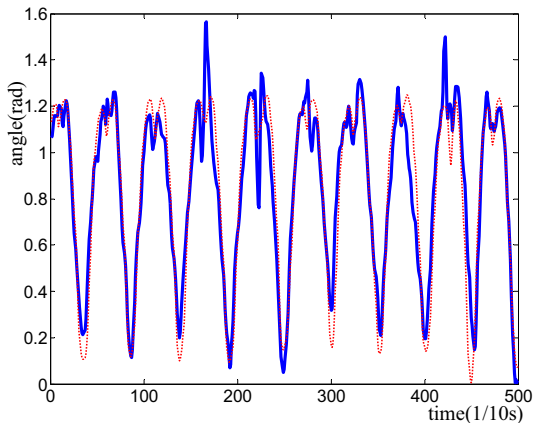


Fig. 6 The joint angles at sagittal plane (The red dot line: the output expected; the blue solid line: the output predicted)

Observing the training and testing results, the errors on y-axis were found to be larger than the others. The x-, y- and

z-axis in the experiment were vertical to the traverse, sagittal and frontal plane, respectively. The flexion and extension motion mainly lay in the sagittal plane, so the motion on y-axis was very weak. Moreover, the muscle activation at biceps and triceps was not significantly related to the motion on y-axis. In conclusion, the error on y-axis could be ignored during evaluating the CPG model. The error on z-axis was obviously larger than that on x-axis, which was caused by the backarm swing on z-axis. The backarm swing was determined by the muscle on shoulders and independent on biceps or triceps. The forearm extension may be a freely falling action because of gravity, and the sEMG at triceps was very weak. So the sEMG at triceps muscles had little help in recognizing the extension angle of forearms.

The output data of our CPG model indicated the motion trajectory for robot control. An exoskeleton robot [23] was controlled with these outputs as shown in Fig. 7. The robot provided a rotation DOF in sagittal plane at the elbow joint. The output data were reduced into two dimensions with principal component analysis, and then were resolved as angles in sagittal plane. A maxon motor was controlled to follow the angle sequence with a simple PID strategy. The output trajectory was recorded by an encoder in the motor and shown in Fig. 8. The Fig. 8 demonstrated that the CPG model could be applied in robot control. The real curve in Fig. 7 did not closely follow the aim trajectory, and the main reason we thought that, was the PID parameter had not been adjusted perfectly. The angle sequence was about 10Hz, and a smooth interpolation must be helpful to better control effect.

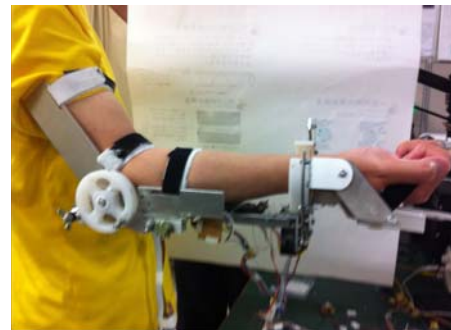


Fig. 7 An exoskeleton robot

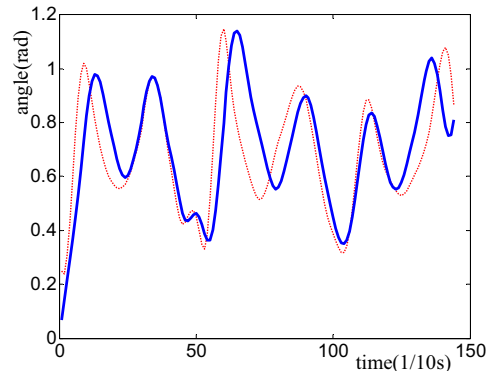


Fig. 8 The motion trajectory of the robot (The red dot line: aim trajectory; the blue solid line: real trajectory)

IV. CONCLUSIONS

This study aims at more intelligent robots not apart from human manipulation. The higher intelligence means to be the more powerful autonomous and poorer controllable. A new modulatable CPG model was presented in this paper for robot control. Our CPG model was oriented to balance the trade-off between the autonomous and controllable features.

The CPG model was built based on an ESN, which could learn the human motion pattern from training data. The training data included sEMG signals and motion position sampled synchronously. SEMG signals were used as the input of ESNs and motion position as output. The trained ESN could output the motor commands like an oscillator, and these commands were under the control of human's sEMG. The trained ESN could be embedded into robots as a CPG, and then the robots worked under human control.

Our CPG model is different from the traditional oscillator models. It has more complex dynamics, can easily output high dimensional motion data, and its parameters are determined by supervised learning. Our CPG model is different from the motion intention recognition based on neural networks. There are not any processing like feature extraction and pattern classification during building the model. Of course, our model can be considered as temporal pattern recognition distinct from the common statistical pattern recognition. Our CPG model is different from a neuron-musculo-skeletal model. It focuses on capturing the dynamics in the mapping from sEMG to motion, not seeking the mapping function itself. So the CPG model can autonomously output novel motor commands according to the dynamics learned from training data, and the autonomous output is restricted by sEMG coming from humans.

This paper has illustrated the CPG model can learn the frequency transition from training data, and an instance with sEMG driving is also realized and tested in exoskeletons. But there are many works waiting for being researched in the future.

(1) The frequency modulation may result in the change of the output amplitude, but no reasonable interpretations could be provided.

(2) A more smooth and quick estimation for sEMG amplitude is needed. The smooth input can avoid the noise to be introduced into the model output. A quick estimating method can help us in real time control.

(3) When a robot is controlled with our CPG model, it is hard to respond to the perturbations of environments, because the CPG model has not accepted any feedback from environments.

(4) The robot controlled by CPG models is not on passive status in human robot interaction. The robot's dynamics is a new unstable factor in interaction systems.

REFERENCES

- [1] E. Marder and D. Bucher, "Central pattern generators and the control of rhythmic movements," *Curr Biol.*, vol. 11, no. 23, pp. R986-96. Nov. 2001.
- [2] A. J. Ijspeert, "Central pattern generators for locomotion control in animals and robots: a review," *Neural Netw.*, vol. 21, no. 4, pp. 642-653, May. 2008.
- [3] M. Ajalloeian, M. N. Ahmabadi, B. N. Araabi and H. Moradi, "Design, implementation and analysis of an alternation-based central pattern generator for multidimensional trajectory generation," *Robot. Aut. S.*, vol. 60, no. 2, pp. 182-198, Feb. 2012.
- [4] J. Santos and Á. Campo, "Biped locomotion control with evolved adaptive center-crossing continuous time recurrent neural networks," *Neurocomput.*, vol. 86, pp. 86-96, Jun. 2012.
- [5] D. G. Zhang and K.Y. Zhu, "Theoretical analysis on neural oscillator toward bio-mimic robot control," *Int. J. H. Robot.*, vol. 4, no. 4, pp. 1-19, Dec. 2007.
- [6] S. Sukhbaatar, T. Makino, K. Aihara, and T. Chikayama, "Robust generation of dynamical patterns in human motion by a deep belief nets," *J. Mach. Learn. Res.*, vol. 20, pp. 231-246, Nov. 2011.
- [7] J. Li and H. Jaeger, "Minimal energy control of an ESN pattern generator," Jacobs. University technical report No. 26, 2011.
- [8] E. Antonelo, B. Schrauwen and J.V. Campenhout, "Generative modeling of autonomous robots and their environments using reservoir computing," *Neural Proc.*, vol. 26, no. 3, pp. 233-249, Oct. 2007.
- [9] E. A. Antonelo and B. Schrauwen, "Supervised learning of internal models for autonomous goal-oriented robot navigation using reservoir computing," in 2010 *IEEE Int. Conf. on Robotics and Automation*, pp. 2959 - 2964.
- [10] F. Wyffels and B. Schrauwen, "Design of a central pattern generator using reservoir computing for learning human motion," in 2009 *ECSIS Symposium on Advanced Technologies for Enhanced Quality of Life*, , pp. 118-122.
- [11] <http://mocap.cs.cmu.edu/>
- [12] T. Waegeman, F. Wyffels and B. Schrauwen, "A discrete/rhythmic pattern generating RNN," in *Proceedings of the 20th European Symposium on Artificial Neural Networks, Computational Intelligence and Machine Learning*, pp. 567-572.
- [13] A. Pitti, R. Niiyama and Y. Kuniyoshi, "Creating and modulating rhythms by controlling the physics of the body," *Auton. Robot.*, vol. 28, no. 3, pp. 317-329, Apr. 2010.
- [14] R. Ronsse, N. Vitiello, T. Lenzi, J. van den Kieboom, M.C. Carrozza and A.J. Ijspeert, "Human-robot synchrony: flexible assistance using adaptive oscillators," *IEEE Trans. Biomed. Eng.*, vol. 58, no. 4, pp. 1001-1012, Apr. 2011.
- [15] E. Ettore, R. Jacob, C. Joel and B. Stephen, "Real-time myoprocessors for a neural controlled powered exoskeleton arm," *IEEE Trans. Biomed. Eng.*, vol. 53, no. 11, pp. 2389-2396. Nov. 2006.
- [16] O. Fukuda, T. Tsuji, M. Kaneko and A. Otsuka, "A human-assisting manipulator teleoperated by EMG signals and arm motions," *IEEE Robot.*, vol. 19, no. 2, pp. 210-222, Apr. 2003.
- [17] P. K. Artemiadis and K. J. Kyriakopoulos, "A Switching Regime Model for the EMG-based Control of a Robot Arm," *IEEE Syst. B.*, vol. 41, no. 1, pp. 53-63, Feb. 2011.
- [18] D. G. Zhang, P. Poignet, F. Widjaja and W.T. Ang, "Neural oscillator based control for pathological tremor suppression via functional electrical stimulation," *Con. Eng. Pr.*, vol.19, no. 1, pp.74-88, Jan. 2011.
- [19] H. Jaeger and H. Haas, "Harnessing nonlinearity: Predicting chaotic systems and saving energy in wireless communication," *Science*, vol. 304, no. 5667, pp. 78-80, Apr. 2004.
- [20] H. Jaeger, M. Lukosevicius, D. Popovici and U. Siewert, "Optimization and applications of echo state networks with leaky-integrator neurons," *Neural Netw.* vol. 20, no. 3, pp. 335-352, Apr. 2007.
- [21] E. A. Clancy, E. L. Morin and R. Merletti, "Sampling, noise-reduction and amplitude estimation issues in surface electromyography," *J Electromy.*, vol. 12, no. 1, pp. 1-16, Feb. 2002.
- [22] Z. G. Zhang, H. T. Liu, S. C. Chan, K. D. Luk, and Y. Hu, "Time-dependent power spectral density estimation of surface electromyography during isometric muscle contraction: methods and comparisons," *J Electromy.*, vol. 20, no. 1, pp. 89-101, Feb. 2010.
- [23] Z. B. Song and S. X. Guo, "Design process of a novel exoskeleton rehabilitation device and implementation of bilateral upper limb motor movement," *J. Med. Biol. Eng.* (In press.)